AIAA JOURNAL
Vol. 31, No. 7, July 1993

Control of Vortices on a Delta Wing by Leading-Edge Injection

W. Gu,* O. Robinson,* and D. Rockwell†
Lehigh University, Bethlehem, Pennsylvania 18015

This experimental investigation addresses the control of flow past a half-delta wing at high angle of attack. Application of steady blowing, steady suction, or alternate suction-blowing in the tangential direction along the leading edge of the wing can retard substantially the onset of vortex breakdown and stall. The most effective period of the alternate suction-blowing is on the order of one convective time scale of the flow past the wing. As a result of this type of control, the vortex structure in the crossflow plane is modified from a fully stalled condition to a highly coherent leading-edge vortex. This transformation to a restabilized vortex is represented by instantaneous velocity fields, streamline patterns, and vorticity contours.

Nomenclature

A_j = cross-sectional area of jet slit
C = root chord of wing
C_μ = $(V_j/U)^2\,(A_j/S^2)$
$C_{\mu m}$ = maximum value of blowing coefficient for unsteady blowing-suction
f = frequency of periodic suction-blowing
f_s = scanning frequency of laser beam
R = radius of curvature of leading edge of wing
Re = Reynolds number, $U_\infty C/\nu$
S = semispan of wing at trailing edge
T = period of unsteady blowing-suction
t = thickness of wing, time
U = freestream velocity
V_j = steady suction or blowing (tangential) velocity from slip or amplitude of periodic blowing-suction
x_{b0} = initial location of vortex breakdown before application of blowing/suction
Δx_b = location of vortex breakdown in presence of blowing or suction
Δx_{bm} = maximum attainable displacement (in downstream direction) of onset of vortex breakdown during application of blowing or suction
ν = kinematic viscosity

Introduction

At high angle of attack, the flow past delta wings and bodies of revolution exhibits undesirable characteristics such as vortex breakdown, vortex asymmetries, and onset of stall. These characteristics can lead, for example, to loss of control of aircraft undergoing severe maneuvers at high angle of attack. Suitable application of either steady or unsteady injection at the leading edge of the wing or forebody may not only enhance the stability of the leading-edge vortices but also increase the lift/moment on the wing or body.

Steady injection techniques have focused on blowing along, or at, the leading edge of a wing. A variety of blowing configurations have been employed by Bradley et al.,[1] Campbell,[2] Seginer and Salomon,[3] Shi et al.,[4] Wood and Roberts,[5] and Visser et al.[6] The magnitude of the dimensionless momentum coefficient C_μ required to generate a significant alteration of the location of vortex breakdown, lift, or moment varies widely with location and orientation of the steady blowing. In the foregoing investigations, C_μ has an order of magnitude in the range of $10^{-3} \le C_\mu \le 10$. Most relevant to the present study is the investigation of Wood and Roberts,[5] in which the blowing was applied tangentially to a rounded, swept leading edge. Substantial changes in the magnitudes of the surface suction pressure and normal force were attained for values of C_μ on the order of 10^{-2}.

Unsteady injection has been employed in several forms. Periodic blowing-suction applied normal to the leading edge of a delta wing can significantly enhance the coherence of small-scale vortices in the shear layer separating from the leading edge[7]; the possible consequence on the onset of vortex breakdown is unknown. Transient suction along the axis of the vortex allows a delay in the onset of vortex breakdown[8]; the time scale of the vortex response to the imposed transient is a strong function of the steady-state suction amplitude. Unsteady bleed applied to the forebody of conical and cylindrical bodies at high angle of attack can effectively control the forebody vortices and their degree of symmetry.[9-11]

Of course, the effectiveness of these various types of steady and unsteady control techniques applied to delta wings will depend on a number of parameters, including angle of attack, sweep angle, and particulars of the wing geometry including its thickness and leading-edge contour. An assessment of these characteristics, including the effects of sweep angle and leading-edge bluntness on vortex breakdown and stall, in the absence of applied control, is given by Roos and Kegelman.[12] The study of Wood and Roberts[5] shows that an apparent advantage of a blunt, as opposed to a sharp, leading edge is the possibility of substantially altering the location of separation from the leading edge during the application of tangential blowing. The present study addresses this class of delta wings with thick leading edges.

The overall objective of the present investigation is to characterize the instantaneous flow structure formed from the leading edge of a delta wing at high angle of attack, with application of steady and unsteady injection applied tangentially to the leading edge of the wing. Steady blowing, steady suction, and alternating blowing-suction are applied at the leading edge, and their effectiveness on reorganization of the leading-edge vortex is examined. The transient response of the structure of the leading-edge vortex in the crossflow plane is also addressed.

Experimental System and Techniques

Experiments were carried out in a free surface water channel having a width of 914 mm and a height of 610 mm. The entire system was constructed of Plexiglas® to facilitate visualization

Received March 17, 1992; revision received Oct. 12, 1992; accepted for publication Oct. 20, 1992.

*Research Associate.
†Paul B. Reinhold Professor, Department of Mechanical Engineering and Mechanics. Member AIAA.

by dye injection and particle tracking. The test section insert employed for the delta wing configuration consisted of a base plate spanning the width of the channel, having a length of 1235 mm, and elevated a height of 162 mm above the floor of the test section. A half-delta wing was placed on the surface of this base plate. It was held in position by a rotatable disk, which allowed adjustment of the delta wing to arbitrary angle of attack α, as indicated in Fig. 1. The location of dye injection ports on the upstream side of the leading edge of the wing allowed effective visualization of the core of the leading-edge vortex.

An overview of the delta wing configuration is given in Fig. 2. Its chord $C = 457$ mm corresponded to a value of Reynolds number $Re = 1.7 \times 10^4$. The sweep angle λ of the wing was 75 deg. The wing was oriented at an angle of attack $\alpha = 54$ deg, corresponding to the onset of vortex breakdown near the apex of the wing. An inlet line attached to the trailing edge of the wing allowed the injection fluid to pass into a reservoir within the interior of the wing, then out through a thin slit.

A close-up view of the injection slit is indicated in Fig. 3; its configuration produces injection tangential to the leading edge. The radius of curvature of the leading edge of the wing was $R = 9.5$ mm, relative to the wing thickness $t = 19$ mm. The injection slit had a width of 0.76 mm.

To generate various functional forms of injection through the slit of the wing, a piston-type function generator was designed and implemented. In essence, a piston was driven with a defined, time-dependent displacement within a cylindrical tube by means of a computer-controlled stepping motor, which had a resolution on the order of 10,000 steps per revolution. This approach allowed the basic cases of steady blowing and suction, as well as alternate blowing-suction, at arbitrary period and amplitude. A major advantage of employing water as a working fluid is that the time scales are substantially longer than those employed in corresponding air experiments. For this study, the characteristic frequency corresponding to alternating blowing-suction at a period of one convective time scale was $f = U/C = 0.086$ Hz.

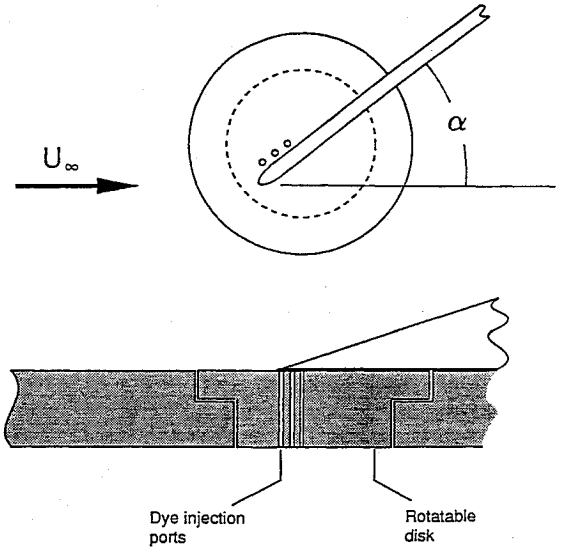

Fig. 1 Plan and side (cross-sectional) views of half-delta wing mounted on base plate and attached to rotatable disk.

Dye visualization involved injection of food coloring mixed with water through the three dye ports illustrated in Fig. 1. Direct particle tracking involved seeding the flow with 4μ metallic-coated particles and illuminating them with a scanning laser sheet. To generate the sheet, a 4-W argon-ion laser operating in the multiline mode was steered onto an oscillating mirror driven at a scanning frequency of $f_s = 80$ Hz by a galvanometer system. Since the time scale of the scanning laser beam was several orders of magnitude smaller than the characteristic time scale of the vortex flow, the viewing camera perceived the particles as instantaneously illuminated at a frequency corresponding to the scanning rate.

Both dye and flow visualization images were acquired using a 35-mm camera that was fired by a computer-controlled system. This system also drove the piston-cylinder arrangement. In this manner, it was possible to obtain photographs at desired instants during steady or unsteady injection. The instantaneous velocities over the crossflow plane were obtained using a direct particle tracking technique; it involved individual inspection of the particle images in conjunction with a digitizing tablet. This approach served as the predecessor and verifier of the fully automated interrogation system of particle image velocimetry.[13]

The response of the core of the vortex to steady blowing, steady suction, and alternate blowing-suction was examined by injecting dye at the leading edge of the wing. In all cases, the control was abruptly initiated at time $t = 0$, and the sequential development in time was photographed until a steady-state condition was attained. At that instant, the control was abruptly terminated, and the return of the vortex core to its initial position was observed. In the present investigation, typically about 1500 velocity vectors were obtained for each realization of the crossflow plane. Use of the adaptive gaussian window (AGW) technique, described in the investigation of Robinson and Rockwell,[14] allowed interpolation of the randomly located velocity vectors to a rectangular grid. Instantaneous streamline patterns and vorticity contours were determined using software developed in our laboratory.

Leading-Edge Vortex Structure: Onset of Vortex Breakdown

Alteration of the onset of vortex breakdown and the corresponding occurrence of the stall process for steady blowing, abruptly applied at $tU/C = 0$, is shown for increasing values of time by the dye visualization sequence in Fig. 4. The onset

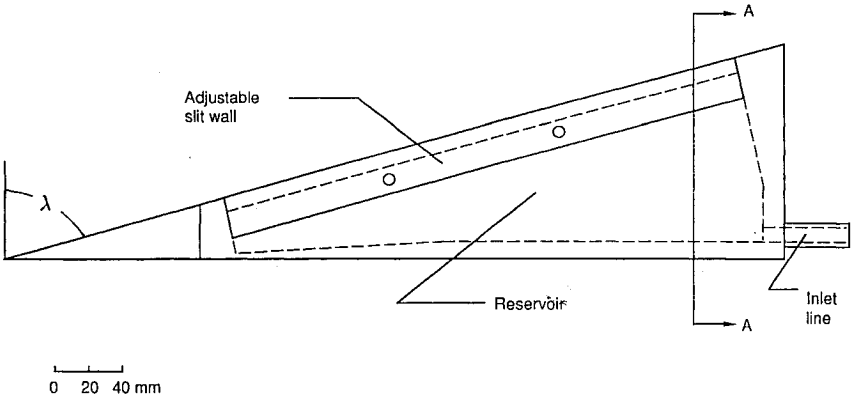

Fig. 2 Overview of half-delta wing showing fluid reservoir within wing that receives steady or unsteady flow from inlet line. Fluid eventually leaves through slit along leading edge of delta wing.

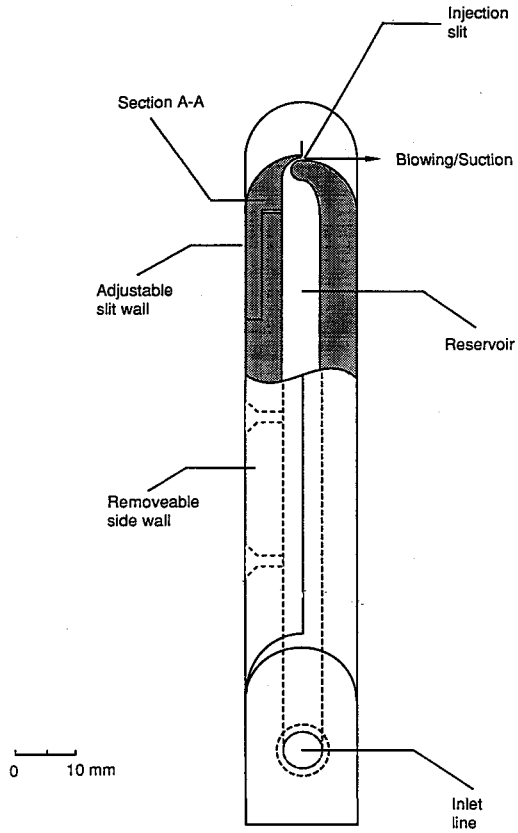

Fig. 3 Cross-sectional (A–A) view of injection slit (compare with Fig. 2) employed for producing either steady or alternating blowing-suction in a direction tangential to the leading edge of the wing.

of vortex breakdown moves downstream at successively larger values of tU/C; at $tU/C = 3.5$, the blowing is abruptly discontinued. Thereafter, the vortex breakdown process relaxes toward its equilibrium position; in the photo at $tU/C = 7.8$, it has not yet attained equilibrium. Considering the overall response of the vortex, it is evident that the downstream movement of vortex breakdown does not occur in a smooth, continuous fashion. Little change occurs over the interval $0 \leq tU/C \leq 0.8$, whereas a very substantial alteration occurs over the time interval $0.8 \leq tU/C \leq 1.7$.

If continuous suction, instead of blowing, is applied, then the corresponding response of the vortex breakdown is as illustrated in Fig. 5. As for the preceding case involving continuous blowing, continuous suction was abruptly started at $tU/C = 0$, then abruptly turned off when the onset of vortex breakdown had moved to its maximum downstream position, represented by the photo at $tU/C = 3.5$. At this instant, the suction is abruptly stopped, and the vortex is allowed to relax to its initial equilibrium position, which is not attained until $tU/C = 22.0$. This relatively long time required for relaxation to the final equilibrium position is associated with a mild overshoot of the vortex breakdown position, i.e., compare visualization photographs at $tU/C = 9.5$ and 0. Concerning the downstream movement of the vortex breakdown position during the time interval $0 \leq tU/C \leq 3.5$, it involves complex changes in the structure of the vortex. For example, in comparing the photograph at $tU/C = 1.7$ with that at 0.8, it is evident that only a minor delay of the onset of vortex breakdown is attained, whereas a large increase occurs over the time interval represented by the dye photographs at $tU/C = 1.7$ and 2.6. In fact, close inspection of the image of $tU/C = 0.8$ suggests three recognizable states in the left, middle, and right regions, respectively: a vortex core in a nonbreakdown (unburst) state, a broken-down (burst) vortex core, and a fully stalled vortex flow. The major change in the flow structure between $tU/C = 0.8$ and 1.7 is a decrease on the cross section of the stall region in the central portion of the image, where the vortex remains in a broken-down (burst) state. Once this transformation occurs, the onset of vortex breakdown moves rapidly downstream, evident by comparing $tU/C = 2.6$ with 1.7.

The case of alternating blowing-suction involves variation of the blowing-suction coefficient C_μ with time t, as illustrated in Fig. 6. The maximum value of this coefficient is designated as $C_{\mu m}$. The horizontal axis of Fig. 6 shows the dimensionless time tU/C from the onset of alternating blowing-suction. For the particular dye visualization shown here, the dimensionless period T of the alternating blowing-suction was $TU/C = 0.77$.

The response of the vortex breakdown and stall processes to the alternating blowing-suction is indicated in the dye visualization series of Fig. 7. At $tU/C = 0$, the oscillatory process is initiated with a suction velocity, as indicated in the C_μ vs t plot of Fig. 6. There is a dramatic downstream movement of the onset of vortex breakdown in the interval $0.8 \leq tU/C \leq 1.7$. The downstream movement of the vortex breakdown occurs, albeit in a noncontinuous fashion, to a dimensionless time $tU/C = 3.9$. At this instant the control is stopped, and there is a mild overshoot involving further downstream movement of the onset of vortex breakdown at $tU/C = 4.8$, then upstream movement of the breakdown toward its equilibrium position. The maximum downstream displacement of the onset of vortex breakdown exceeds that for either the continuous blowing (Fig. 4) or continuous suction (Fig. 5) cases. In fact, this is a general observation over the range of blowing-suction coefficients $C_{\mu m}$ examined in this study.

The classes of response of the leading-edge vortex, as well as the location of onset of vortex breakdown described in Figs. 4, 5, and 7, were found to be generally repeatable from one run to the next. The deviation in location of vortex breakdown is estimated to be $\pm 0.07x_{b0}$.

For the type of alternating blowing-suction described in Figs. 6 and 7, one expects its effectiveness to be a function of both the magnitude of the blowing-suction coefficient $C_{\mu m}$ and the dimensionless period TU/C (or dimensionless frequency fC/U) of the control. Figure 8 shows the maximum downstream displacement Δx_{bm} of the vortex breakdown position normalized with respect to the initial location x_{b0} of vortex breakdown before the onset of oscillatory control as a function of the amplitude of the coefficient $C_{\mu m}$ of the alternating blowing-suction. The most effective amplitude corresponds to $C_{\mu m} = 0.036$. At lower values of $C_{\mu m}$ there is a sharp decrease in the response, whereas for values greater than $C_{\mu m} = 0.036$ the decrease in response is milder.

Figure 9 shows the response of the vortex breakdown displacement $\Delta x_{bm}/x_{b0}$ as a function of the dimensionless forcing frequency fC/U. The response shows a well-defined peak at $fC/U = 1.3$, corresponding to $TU/C = 0.77$. In other words, the optimum period of the alternating blowing-suction corresponds approximately to one convective time scale for optimum displacement of the onset of vortex breakdown.

Figure 10 shows the response of the vortex breakdown displacement $\Delta x_b/x_{b0}$ as a function of the dimensionless time tU/C. The major share of the downstream displacement of the vortex breakdown occurs over a time span of about two convective time scales, i.e., $2C/U$ after onset of the alternating blowing-suction. On cessation of the control, the location of breakdown requires about $3C/U$ to retreat to its initial position. To interpret the local peaks in the response curve, an axis of TU/C is included in the inset; $TU/C = 0$ is aligned with the first peak. Subsequent peaks occur at approximately $TU/C = 1$, 2, and 3. These peaks, however, represent relatively small excursions from the curve representing the general increase in Δx_b. The time scale ($\sim C/U$) of the most effective blowing-suction is substantially less than the time scale of the response of vortex breakdown after application of a transient disturbance such as motion of the wing; the vortex breakdown may require a time as long as $10\text{–}30C/U$ to relax to its new

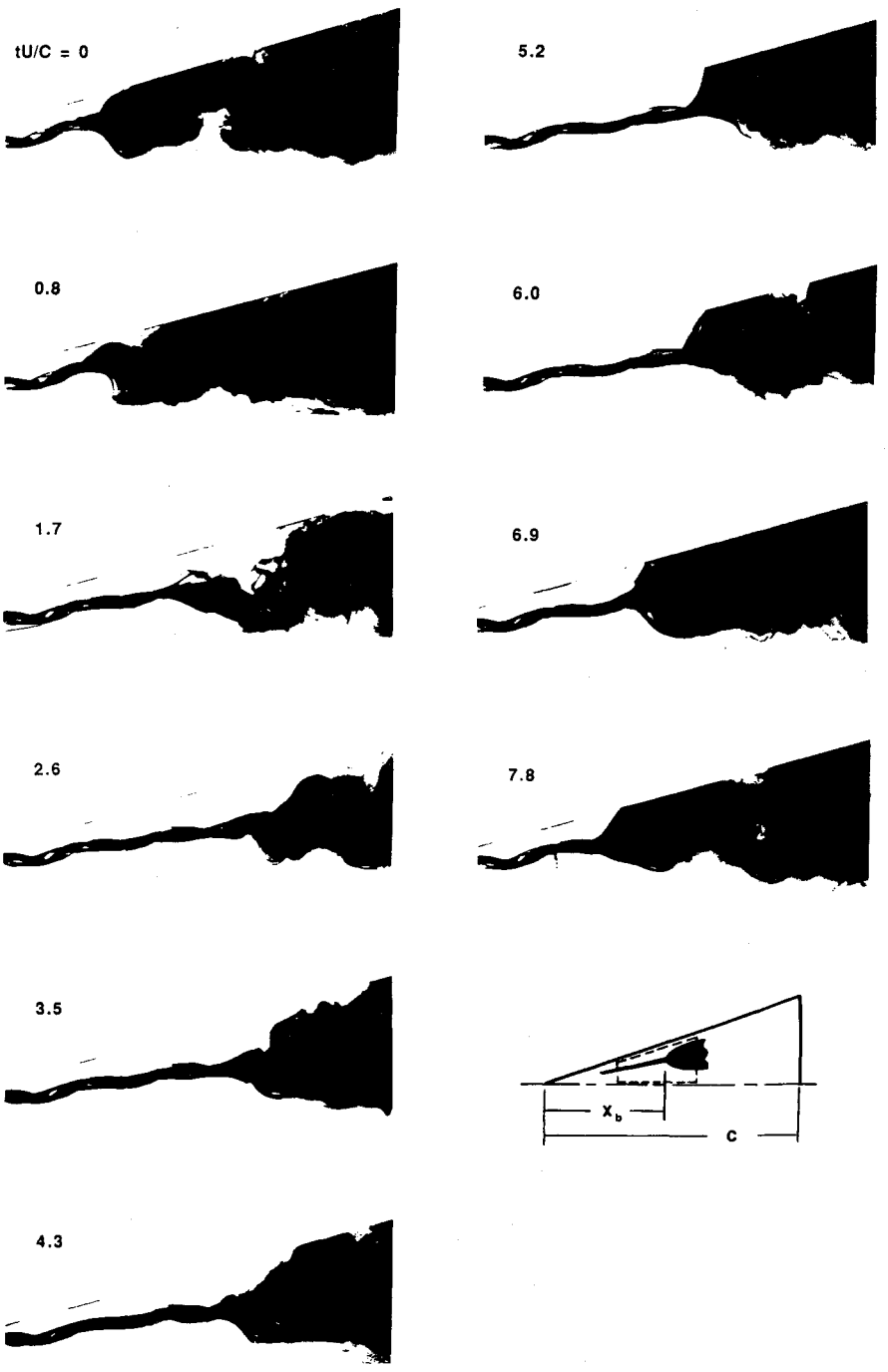

Fig. 4 Dye visualization illustrating alteration of vortex breakdown after onset of steady blowing at time $tU/C = 0$ and abrupt cessation of blowing at $tU/C = 3.5$; blowing coefficient $C_\mu = 0.036$, initial location of onset of vortex breakdown $x_{b0}/C = 0.29$, and maximum downstream displacement of vortex breakdown $\Delta x_b/C = 0.26$.

equilibrium position. This substantial disparity of the time scales of the applied blowing-suction control and the relaxation of the vortex breakdown allows the location of vortex breakdown to be progressively displaced in the downstream direction during continuous application of the unsteady blowing-suction.

Structure of Leading-Edge Vortex in Crossflow Plane During Oscillatory Injection

To characterize the leading-edge vortex in the presence of alternating blowing-suction, described by dye visualization in Fig. 7, instantaneous photographs of particle images were obtained and evaluated in the crossflow plane defined by the arrows in Fig. 7. Evaluation of these images led to the instantaneous velocity fields, streamline patterns, and vorticity distributions described in the following.

Instantaneous Velocity Field in Crossflow Plane

Figure 11 shows the instantaneous velocity field in the crossflow plane at three different times. The schematic at the left in each plot represents the cross section of the half-delta wing. Immediately before the onset of alternating blowing-suction, there is a lack of a coherent leading-edge vortex over the crossflow plane, as illustrated in Fig. 11a. With the exception of a relatively large vortical structure in the separating shear layer from the leading edge, there is no clearly identifiable pattern.

After two complete cycles of the alternating blowing-suction, the instantaneous velocity field takes the form shown in

Fig. 11b. A large-scale, single vortical structure is identifiable, but it is clearly biased toward the lower part of the flow domain. Its approximate center is designated by the bold dot.

At the end of four cycles of the alternating blowing-suction, shown in Fig. 11c, the velocity field of the leading-edge vortex exhibits a highly coherent form, and its center, indicated by the bold dot, has moved upward by a substantial amount from its location in Fig. 11b.

Viewing together the flow patterns shown in Figs. 11b and 11c, a stagnation point occurs along the bottom wall at the location indicated by the arrow. The location of this stagnation point shifts by only a small amount when the apparent center of the vortex undergoes a large displacement.

Contours of Constant Vorticity

Contours of instantaneous vorticity at five different times are given in Figs. 12a–12e. As shown in Fig. 12a, before the onset of control, the major share of vorticity is concentrated in the shear layer separating from the leading edge. A minor concentration is evident in the lower left corner of the crossflow plane. In contrast, in Fig. 12b, the vorticity distribution has started to take the general form of, and in Fig. 12c closely resembles, that in the crossflow plane on a swept wing at low angle of attack, as described by Hoeijmakers.[15]

The issue arises as to how the contours of constant vorticity are modified during successive instants of an oscillation cycle, after a nominally stable vortex has been attained. To examine

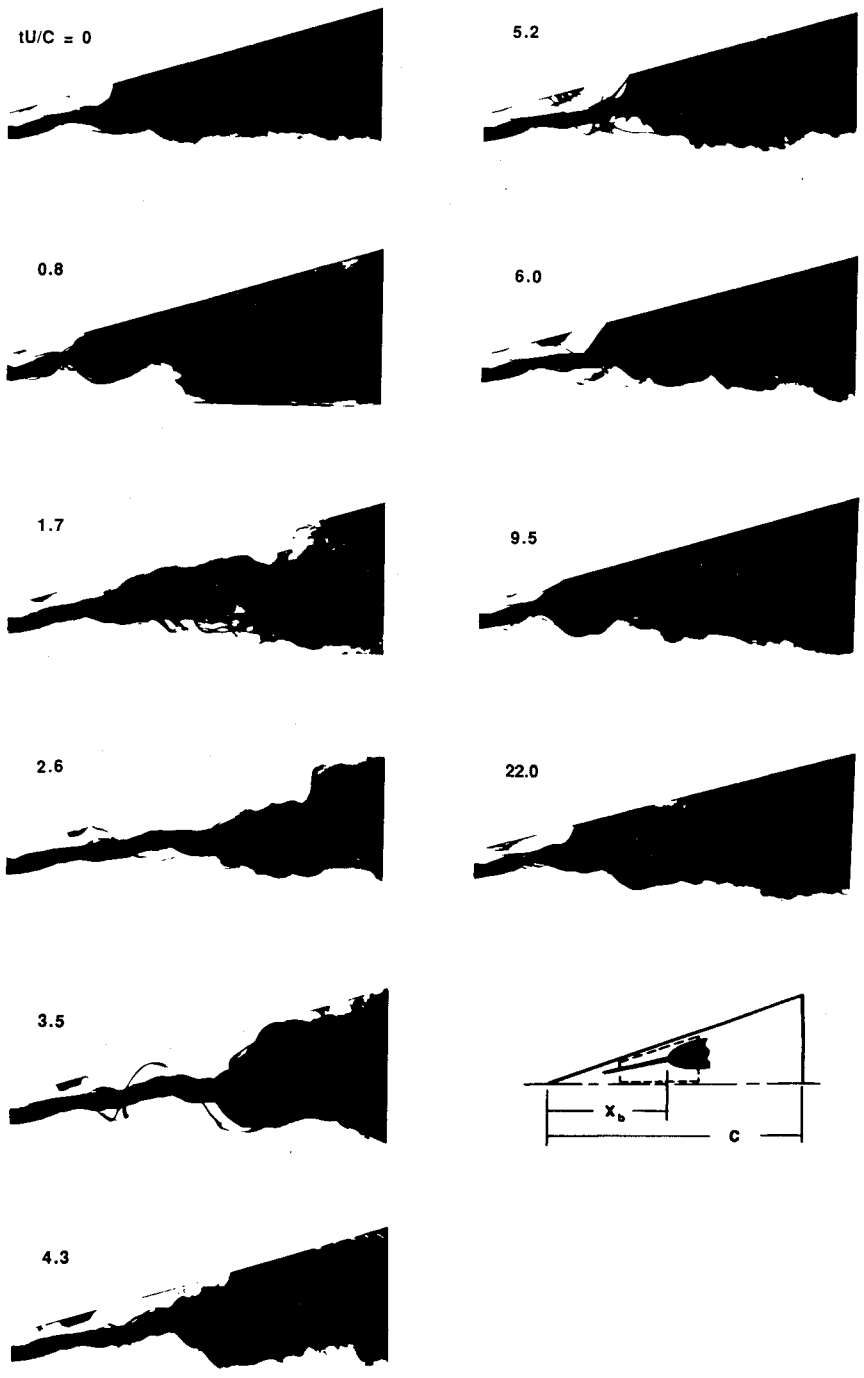

Fig. 5 Dye visualization showing alteration of vortex breakdown after onset of steady suction at time $tU/C = 0$ and abrupt cessation of suction at $tU/C = 3.5$; suction coefficient $C_\mu = -0.036$, initial location of onset of vortex breakdown $x_{b0}/C = 0.29$, and maximum downstream displacement of vortex breakdown $\Delta x_b/C = 0.35$.

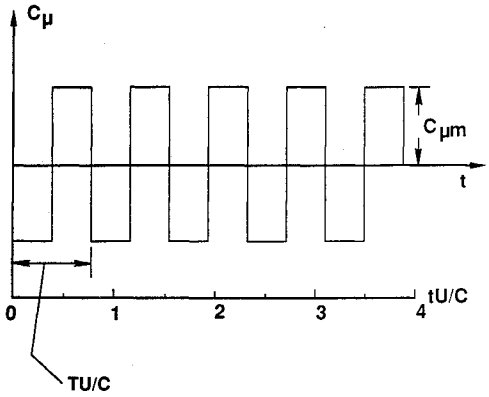

Fig. 6 Schedule for alternating blowing-suction showing momentum coefficient C_μ as a function of dimensionless time tU/C and dimensionless period TU/C.

this response, we consider instants of time well after the onset of the alternate suction-blowing, corresponding to points c, d, and e in Fig. 12. By comparing Figs. 12c–12e, it is possible to observe the change in locus of the center of the vorticity concentration at instants corresponding, respectively, to zero C_μ (point 13), maximum negative C_μ (point 14), and maximum positive C_μ (point 15).

In going from zero to the maximum negative value of C_μ (compare Figs. 12c and 12d), the concentration of vorticity moves down and toward the surface of the wing. It is hypothesized that the suction of fluid away from the portion of the vortex adjacent to the wing draws it closer to the wing surface. This aspect is addressed subsequently in discussion of the corresponding streamline.

On the other hand, onset of the maximum positive C_μ, corresponding to the blowing portion of the alternating blowing-suction (Fig. 12e), moves the center of the concentration of vorticity away from the wing surface.

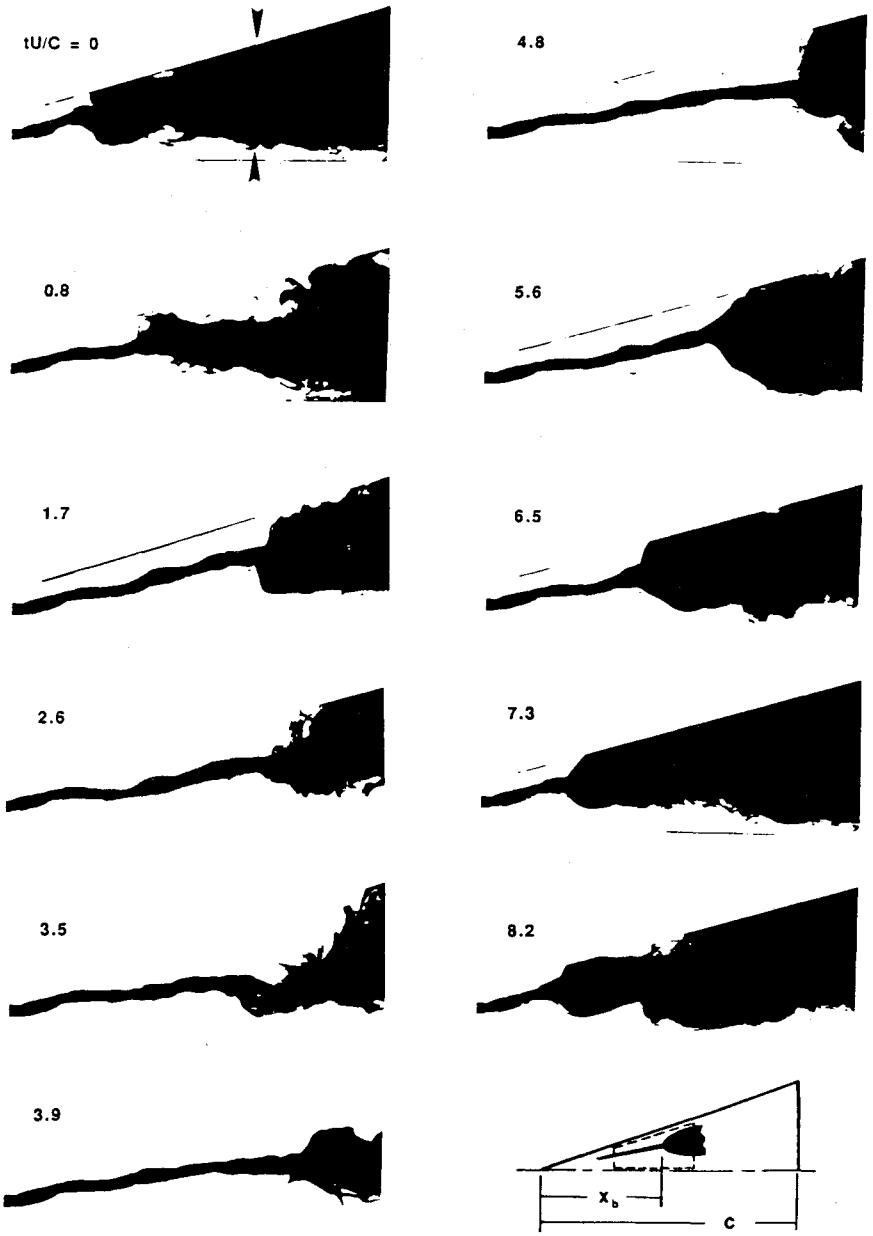

Fig. 7 Dye visualization illustrating alteration of vortex breakdown after onset of alternating blowing-suction at time $tU/C = 0$ and abrupt cessation of blowing at $tU/C = 3.9$; blowing coefficient $C_\mu = 0.036$, initial location of onset of vortex breakdown $x_{b0}/C = 0.29$, maximum downstream displacement of vortex breakdown $\Delta x_b/C = 0.43$, dimensionless period of alternating blowing-suction $TU/C = 0.77$, and amplitude of alternating blowing-suction $C_{\mu m} = 0.036$.

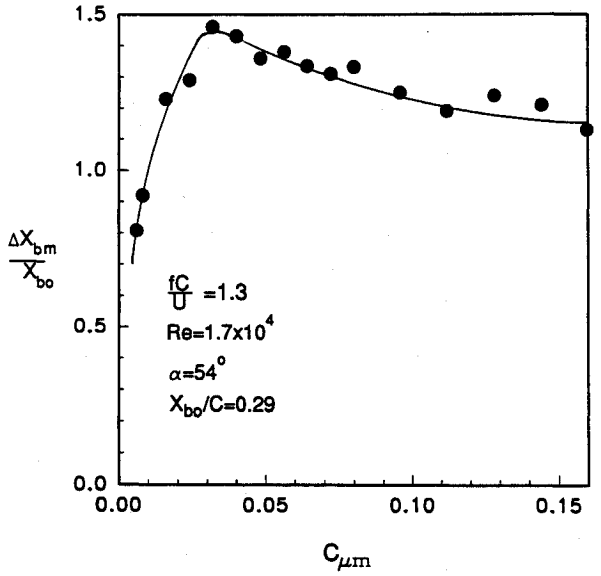

Fig. 8 Maximum attainable downstream displacement Δx_b of onset of vortex breakdown normalized with respect to location x_{b0} of vortex breakdown in absence of alternating blowing-suction vs amplitude of alternating blowing-suction coefficient $C_{\mu m}$; dimensionless frequency and period of alternating blowing-suction are $fC/U = 1.3$ and $TU/C = 0.77$.

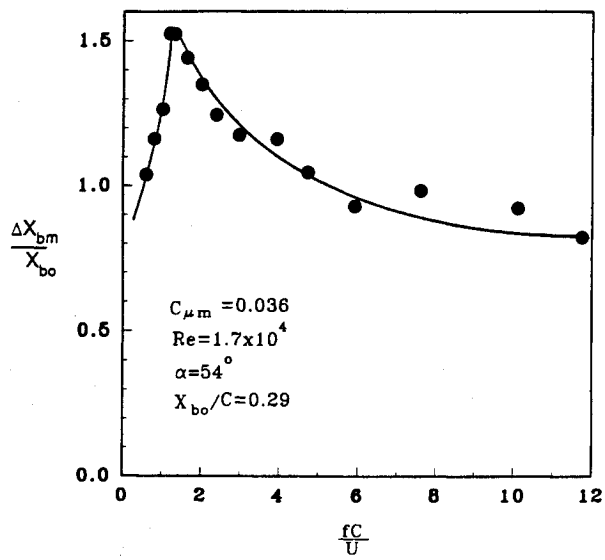

Fig. 9 Maximum attainable (downstream) displacement Δx_b normalized by location x_{b0} of onset of vortex breakdown in absence of alternating blowing-suction as a function of dimensionless frequency fC/U of injection.

Despite the changes in location of the centers of concentration of vorticity in Figs. 12b–12d, the general form of the concentrations remains the same. It is the same as that occurring on a delta wing at low angle of attack.[15] We therefore conclude that once the leading-edge vortex has been stabilized through persistence of the alternating blowing-suction, the stable form of its vorticity distribution is maintained except for variations in instantaneous position of the center of concentration of vorticity.

In Figs. 12b–12e, small-scale concentrations of vorticity appear around the periphery of the large-scale leading-edge vortex. These concentrations are particularly evident in Figs. 12b and 12d. It is hypothesized that they are due to amplification of the Kelvin-Helmholtz instability in the shear separating from the leading edge.

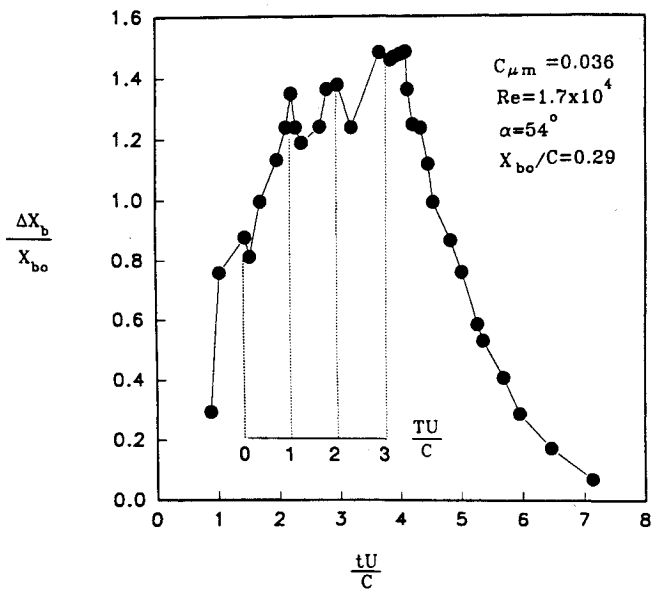

Fig. 10 Downstream displacement Δx_b of onset of vortex breakdown normalized with respect to location x_{b0} of vortex breakdown in absence of alternating blowing-suction vs dimensionless time tU/C of injection; dimensionless period of alternating blowing-suction is $TU/C = 0.77$.

Instantaneous Streamlines

The instantaneous streamline patterns corresponding to successive cases of zero C_μ, maximum negative C_μ, and maximum positive C_μ are illustrated, respectively, in Figs. 13a–13c.

The instantaneous streamline pattern of Fig. 13a, taken at an instantaneous value of $C_\mu = 0$, shows a clearly defined stagnation point on the (horizontal) wall orthogonal to the wing. Moreover, the center of the vortex spirals outward. In the terminology of critical point theory, this type of vortex center is referred to as an unstable focus.[13,16] Such unstable foci have been observed in the nominally two-dimensional vortex street from a stationary, inclined plate by Steiner and Perry[16] and in the leading-edge vortex on a delta wing pitching to high angle of attack by Magness et al.[13] Another feature of the streamline pattern of Fig. 12a is the fact that the separation line from the leading edge does not wind into the vortex; instead, it forms a separation line between the outer irrotational flow and the outward-spiraling vortical flow. This feature also has been observed on a delta wing pitching to high angle of attack by Magness et al.[13] In essence, the existence of an unstable focus suggests that the streamwise structure of the leading-edge vortex along the wing is undergoing a process of contraction, corresponding to deceleration in the region of the core.

During subsequent instants of the alternating blowing-suction process, represented by maximum negative C_μ in Fig. 13b and maximum positive C_μ in Fig. 13c, the same principal features of the leading-edge vortex structure are retained. The location of the stagnation point on the (horizontal) wall orthogonal to the leading edge of the wing remains virtually unchanged. This insensitivity of the stagnation point location is in contrast to the change in the trajectory of the separation streamline emanating from the leading edge of the wing; it is substantially closer to the wing surface for the blowing part of the cycle shown in Fig. 13c.

The details of the streamline pattern for the suction portion of the alternating blowing-suction cycle, shown in Fig. 13b, are relatively complex. A node line N separates the streamlines oriented in the upstream direction and corresponding to fluid sucked into the injection slit and the streamlines spiraling outward from the center of the vortex and moving in the downstream direction. Moreover, there exists a half-saddle point at location S that accommodates fluid sucked into the

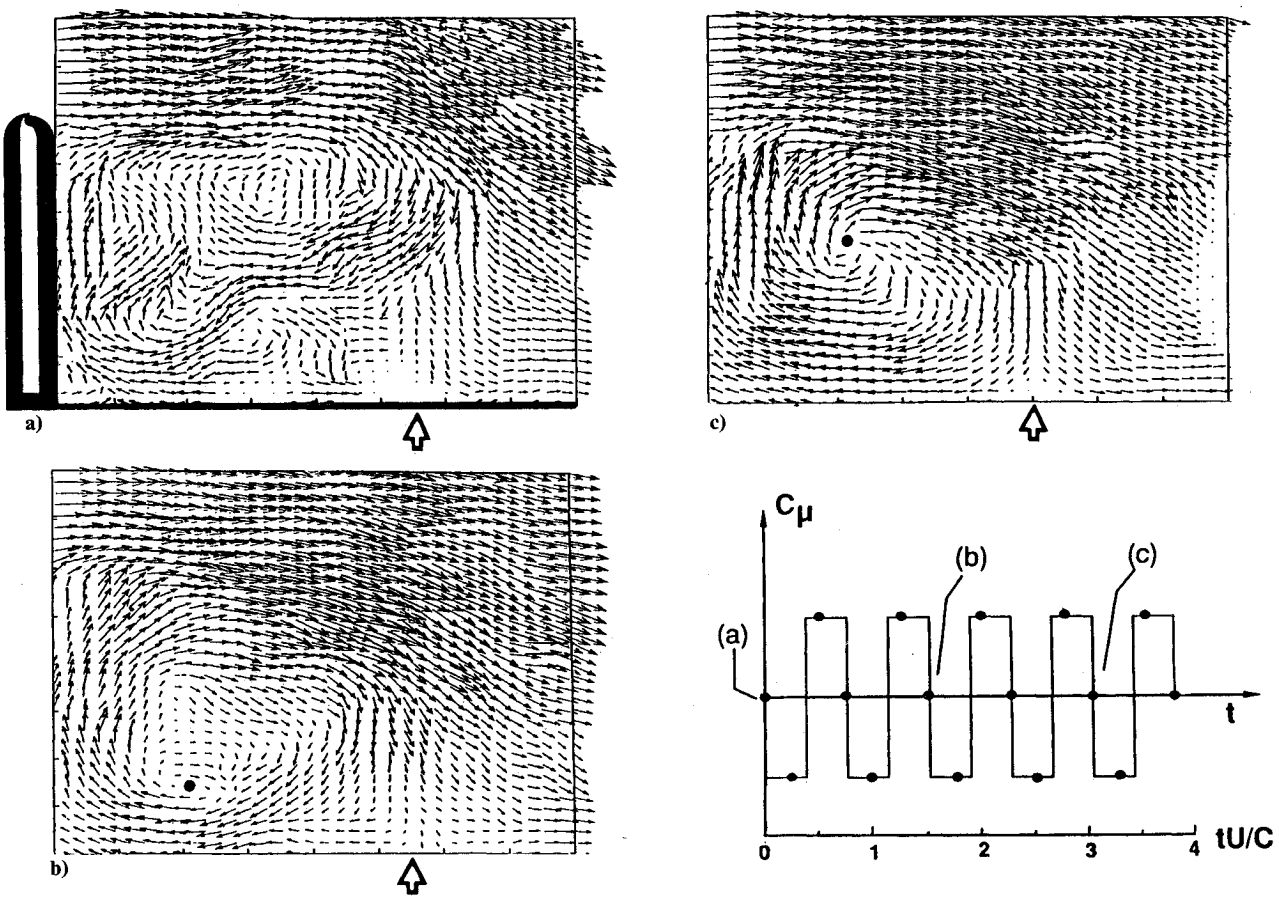

Fig. 11 Instantaneous velocity distribution over crossflow plane on half-delta wing corresponding to a) fully stalled condition in absence of alternating blowing-suction, b) flow structure after two complete cycles of alternating blowing-suction, and c) flow structure after four complete cycles of alternating blowing-suction; period of alternating blowing-suction is $TU/C = 0.77$ and amplitude of alternating blowing-suction is $C_{\mu m} = 0.036$. Black dot indicates apparent center of vortex.

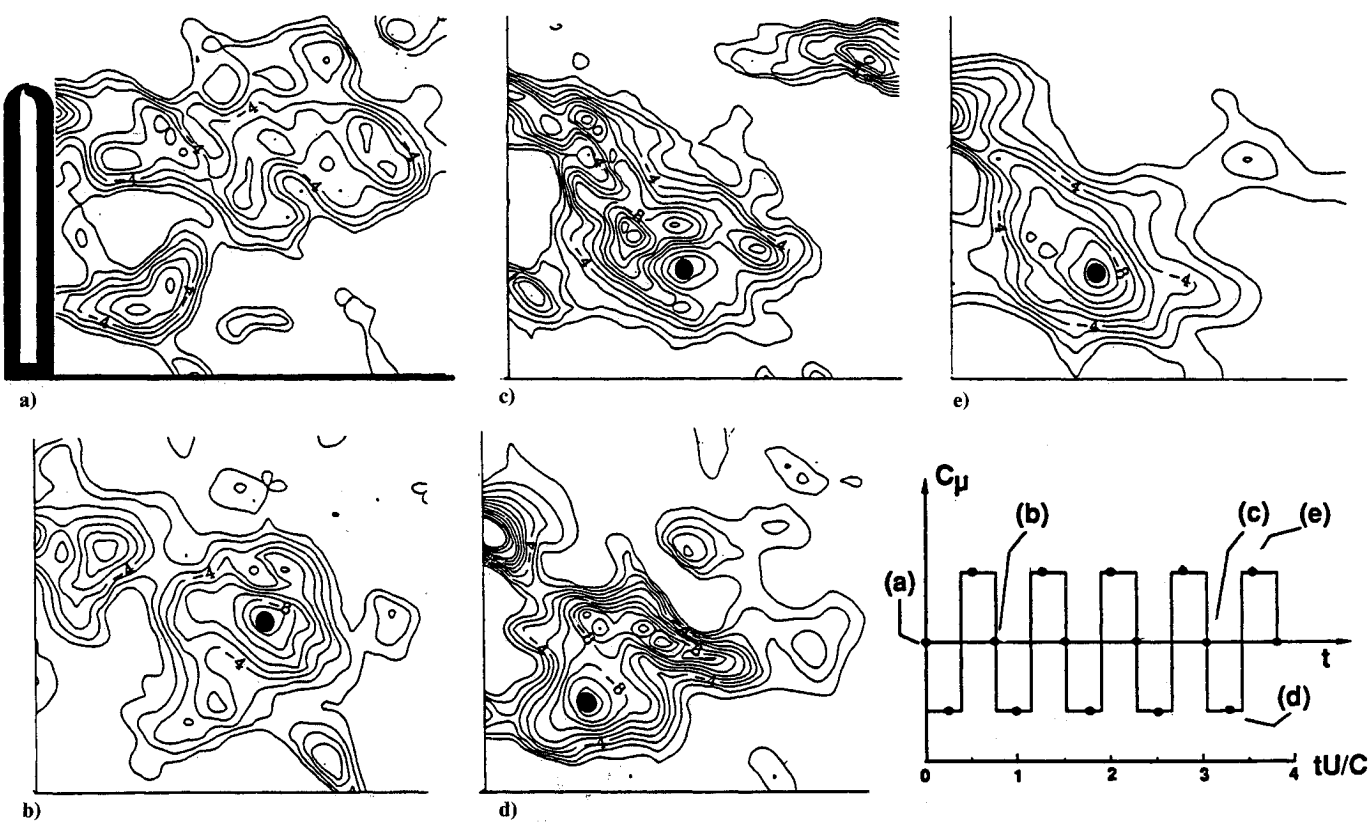

Fig. 12 Instantaneous contours of constant vorticity over crossflow plane of half-delta wing at instant a) immediately before onset of alternating blowing-suction, b) corresponding to completion of one cycle, c) corresponding to completion of four cycles, and d) and e) immediately after completion of four cycles; period of alternating blowing-suction is $TU/C = 0.77$ and amplitude of injection coefficient is $C_{\mu m} = 0.036$.

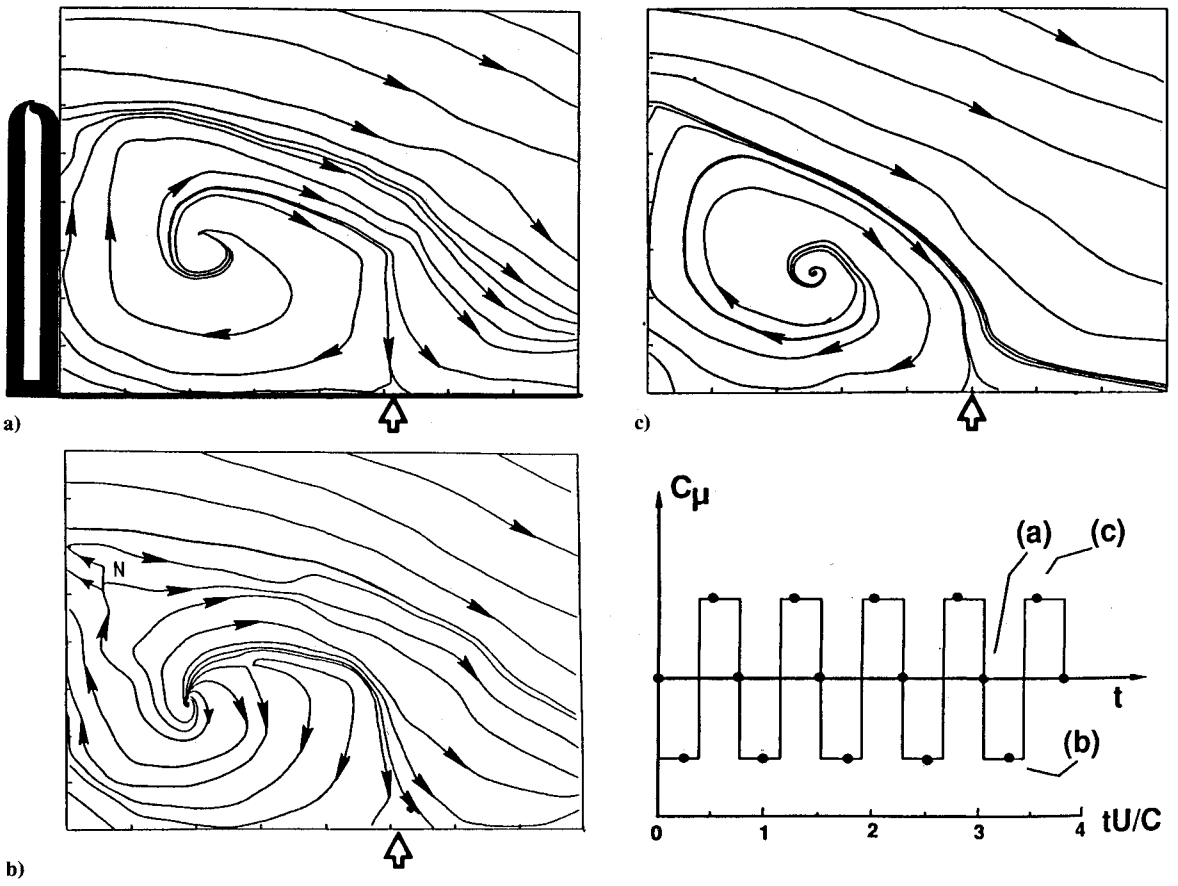

Fig. 13 Instantaneous streamlines over crossflow plane of half-delta wing at instants of a) zero, b) maximum negative, and c) maximum positive blowing, respectively; period of alternating blowing-suction is $TU/C = 0.77$ and amplitude of injection coefficient is $C_{\mu m} = 0.036$.

slit in the upstream direction and moving in the downstream direction away from the center of the vortex.

Concluding Remarks

Tangential injection from the leading edge of a delta wing, in the form of steady blowing, steady suction, or alternating blowing-suction, can retard substantially the onset of vortex breakdown and stall. In general, alternating blowing-suction produces the largest downstream displacement of the vortex breakdown. Once this maximum downstream displacement is attained, it is maintained in a relatively steady position except for small fluctuations. In other words, an essentially steady, downstream displacement of the onset of vortex breakdown can be maintained, irrespective of whether steady blowing, steady suction, or alternating blowing-suction is applied.

In the case of alternating blowing-suction, the maximum downstream displacement of vortex breakdown as a function of time scale of the applied control exhibits a resonant response. Maximum displacement is attained when the period of the alternating blowing-suction is about one convective time scale C/U. The dependence of the displacement of vortex breakdown on the amplitude of the alternating blowing-suction also exhibits a similar resonant response. Significant downstream displacements of the vortex breakdown can be obtained for values of momentum coefficient C_μ on the order of 10^{-2}.

Because of the foregoing events, the structure of the vortex in a given crossflow plane varies as a function of time. It is possible, with proper application of alternating blowing-suction, to drive the leading-edge vortex from a fully broken down, stalled pattern to a stable and coherent vortical structure. The streamline patterns of the stabilized vortex exhibit an outward-spiraling motion near the vortex center, corresponding to an unstable focus within the context of critical point theory. Correspondingly, the separation streamline from the leading edge of the wing partitions the outward-spiraling vortical flow from the irrotational flow exterior to the wing.

Acknowledgments

The authors are pleased to acknowledge the financial support of the Air Force Office of Scientific Research. The contract monitor for this research program is Daniel Fant.

References

[1]Bradley, R. G., Whitten, P. D., and Wray, W. O., "Leading-Edge Vortex Augmentation in Compressible Flow," *Journal of Aircraft*, Vol. 13, No. 4, 1976, pp. 238–242.

[2]Campbell, J. F., "Augmentation of Vortex Lift by Spanwise Blowing," *Journal of Aircraft*, Vol. 13, No. 9, 1976, pp. 727–732.

[3]Seginer, A., and Salomon, M., "Augmentation of Fighter Aircraft Performance by Spanwise Blowing over the Wing Leading Edge," NASA TM 84330, March 1983 (also AGARD-CP-341 Paper 33).

[4]Shi, Z., Wu, J. M., and Vakili, A. D., "An Investigation of Leading-Edge Vortices with Jet Blowing," AIAA Paper 87-0330, Jan. 1987.

[5]Wood, N. J., and Roberts, L., "The Control of Vortical Lift on Delta Wings by Tangential Leading-Edge Blowing," AIAA Paper 87-0158, Jan. 1987.

[6]Visser, K. D., Iwanski, K. T., Nelson, R. C., and Ng, T. T., "Control of Leading-Edge Vortex Breakdown by Blowing," AIAA Paper 88-0504, Jan. 1988.

[7]Gad-el-Hak, M., and Blackwelder, R. F., "Control of the Discrete Vortices from a Delta Wing," *AIAA Journal*, Vol. 25, No. 8, 1987, pp. 1042–1049.

[8]Parmenter, K., and Rockwell, D., "Transient Response of Leading-Edge Vortices to Localized Suction," *AIAA Journal*, Vol. 28, No. 6, 1990, pp. 1131, 1132.

[9]Williams, D. R., El-Khabiri, S., and Papazian, H., "Control of Asymmetric Vortices Around a Cone-Cylinder Geometry with Unsteady Base Bleed," AIAA Paper 89-1004, March 1989.

[10]Williams, D. R., and Papazian, H., "Forebody Vortex Control for the Unsteady Bleed Technique," *AIAA Journal*, Vol. 29, No. 5, 1991, pp. 853–855.

[11]Williams, D., and Bernhardt, J., "Proportional Control of Asymmetric Forebody Vortices with the Unsteady Bleed Technique," AIAA Paper 90-1629, June 1990.

[12]Roos, F. W., and Kegelman, J. T., "Recent Explorations of Leading-Edge Vortex Flowfields," *High Angle of Attack Technology*, NASA CP-3149, Vol. 1, Pt. 1, 1992, pp. 157–172.

[13]Magness, C., Robinson, O., and Rockwell, D., "Instantaneous Topology of the Unsteady Leading-Edge Vortex at High Angle of Attack," *AIAA Journal* (to be published).

[14]Robinson, O., and Rockwell, D., "Construction of Three-Dimensional Images of Flow Structure via Particle Tracking Techniques," *Experiments in Fluids*, Vol. 14, pp. 257–270.

[15]Hoeijmakers, H. W. M., "Methods of Numerical Simulation for Leading-Edge Vortex Flow," *Studies of Vortex-Dominated Flows*, edited by M. Y. Hussaini and M. D. Salas, Springer-Verlag, New York, 1985, pp. 223–269.

[16]Perry, A. E., and Steiner, T. R., "Large-Scale Vortex Structures in Turbulent Wakes Behind Bluff Bodies, Pt. 1, Vortex Formation," *Journal of Fluid Mechanics*, Vol. 174, 1987, pp. 233–270.